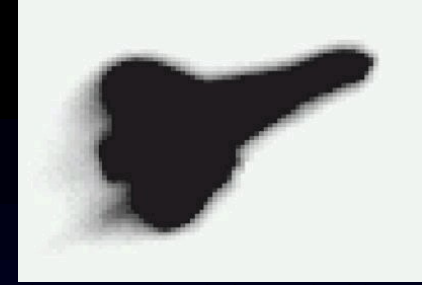


Achieving high resolution

- Diffraction-limited performance with single telescopes with Adaptive Optics
- Or sparse aperture masking
 - Use masks to sub-divide telescope primary into a number of subapertures which are combined interferometrically
 - <http://www.eso.org/sci/publications/messenger/archive/no.146-dec11/messenger-no146-18-23.pdf>
- Interferometry with 2 or more separated telescopes where the resolution depends on λ/b where b is the maximum baseline between apertures
- Plus: lunar occultations, speckle interferometry....

Adaptive Optics



The Space Shuttle imaged with
AO from the Starfire Optical
Range, Phillips AFB, NM

Proposed by Horace Babcock in 1953.

“The Possibility of Compensating Astronomical Seeing”

Developed by US military for satellite observations from the ground, and laser beam propagation.

Astronomical developments in the 1990s as control systems evolved.

Now important in medical imaging and microscopy:

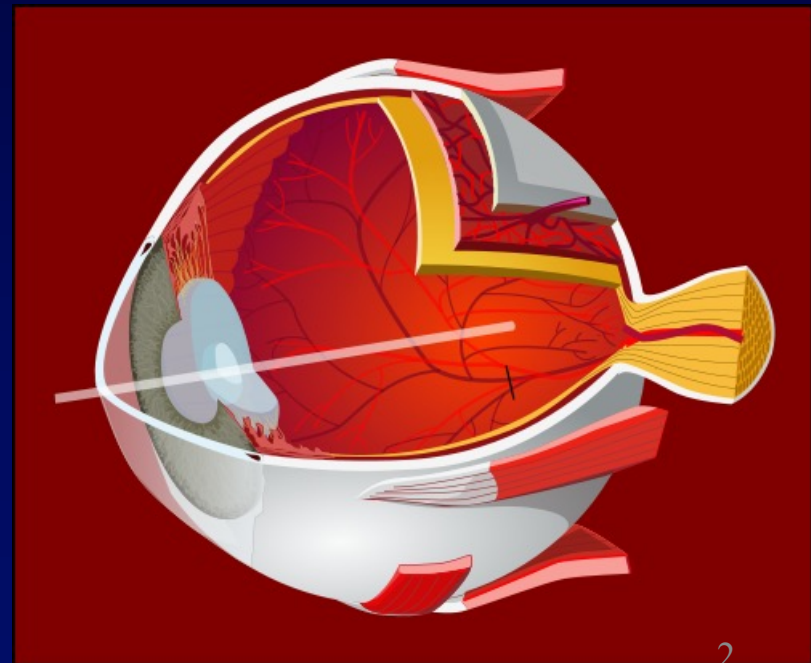
Imaging and spectroscopy of the retina, lens and cornea:

Diagnosis of diseases of the eye

**Diabetic Retinopathy
Macular degeneration**

.....

Window into the circulation and nervous system

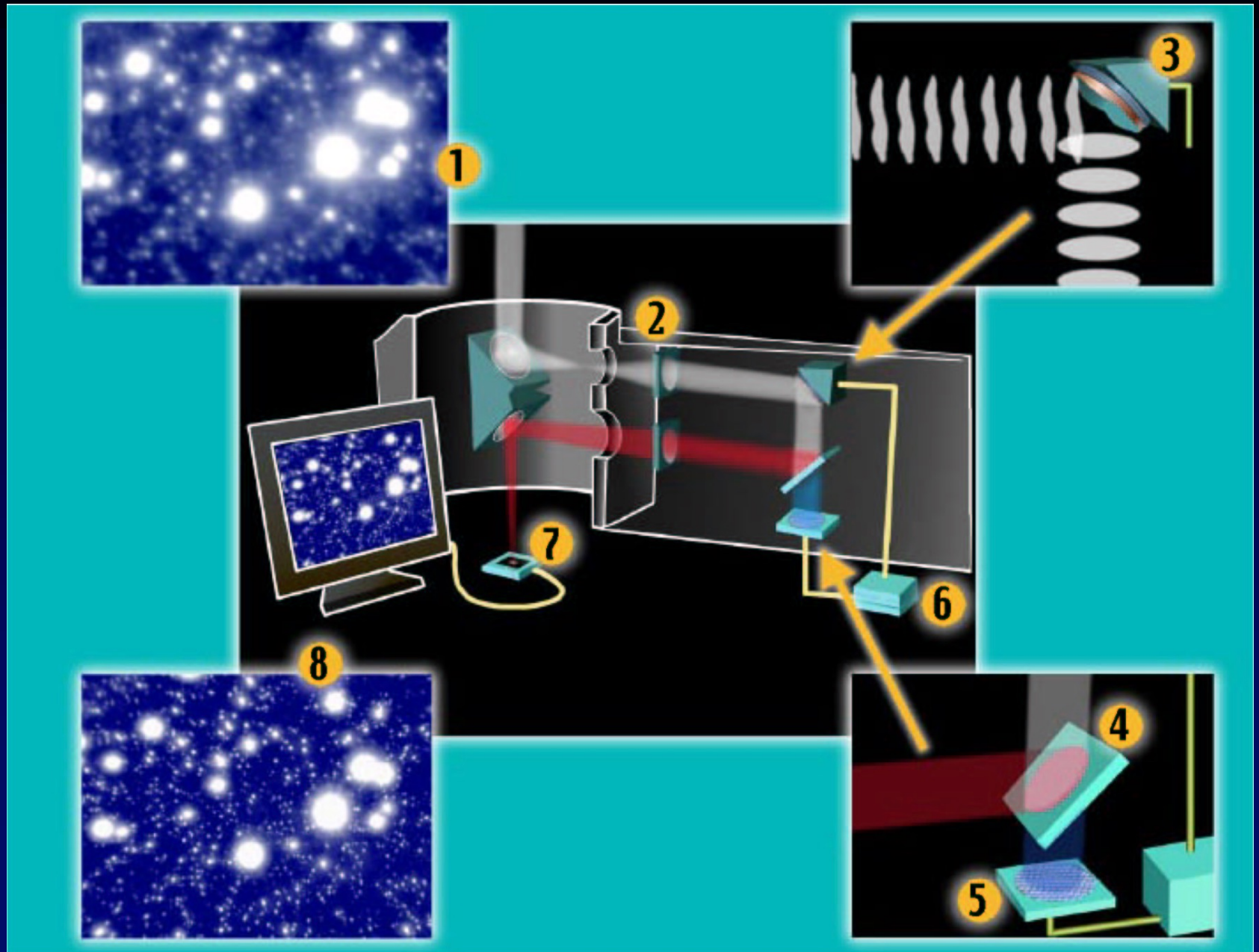


Adaptive Optics in Astronomy

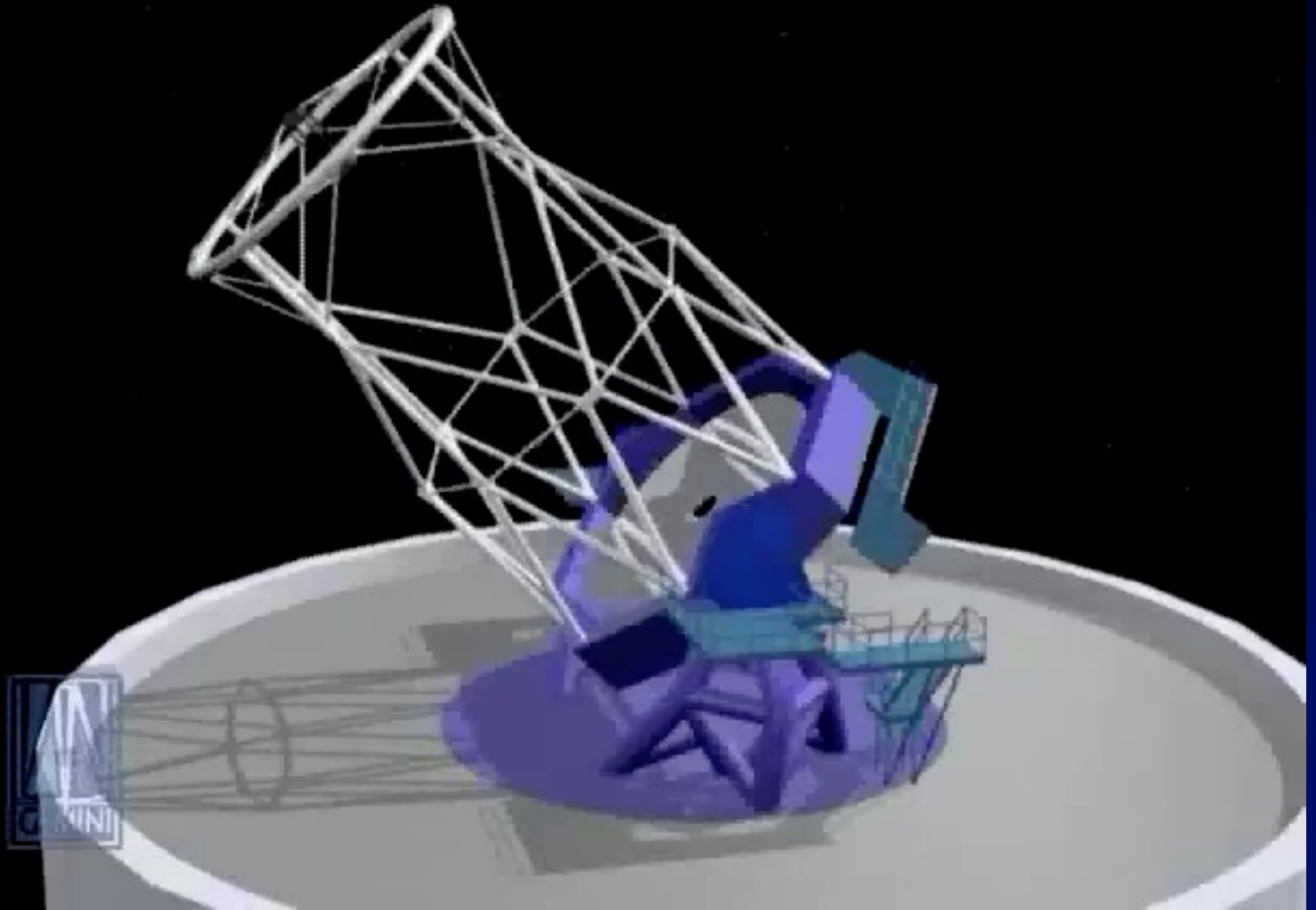
- Real time compensation for atmospheric turbulence
- Restoring near-diffraction-limited performance at infrared wavelengths
- Now pushing image improvements to shorter wavelengths, larger fields, better and more stable image quality
- For detailed tutorials see.

Claire Max: <https://www.ucolick.org/~max/289/>

Adaptive optics to the rescue



How does AO work?

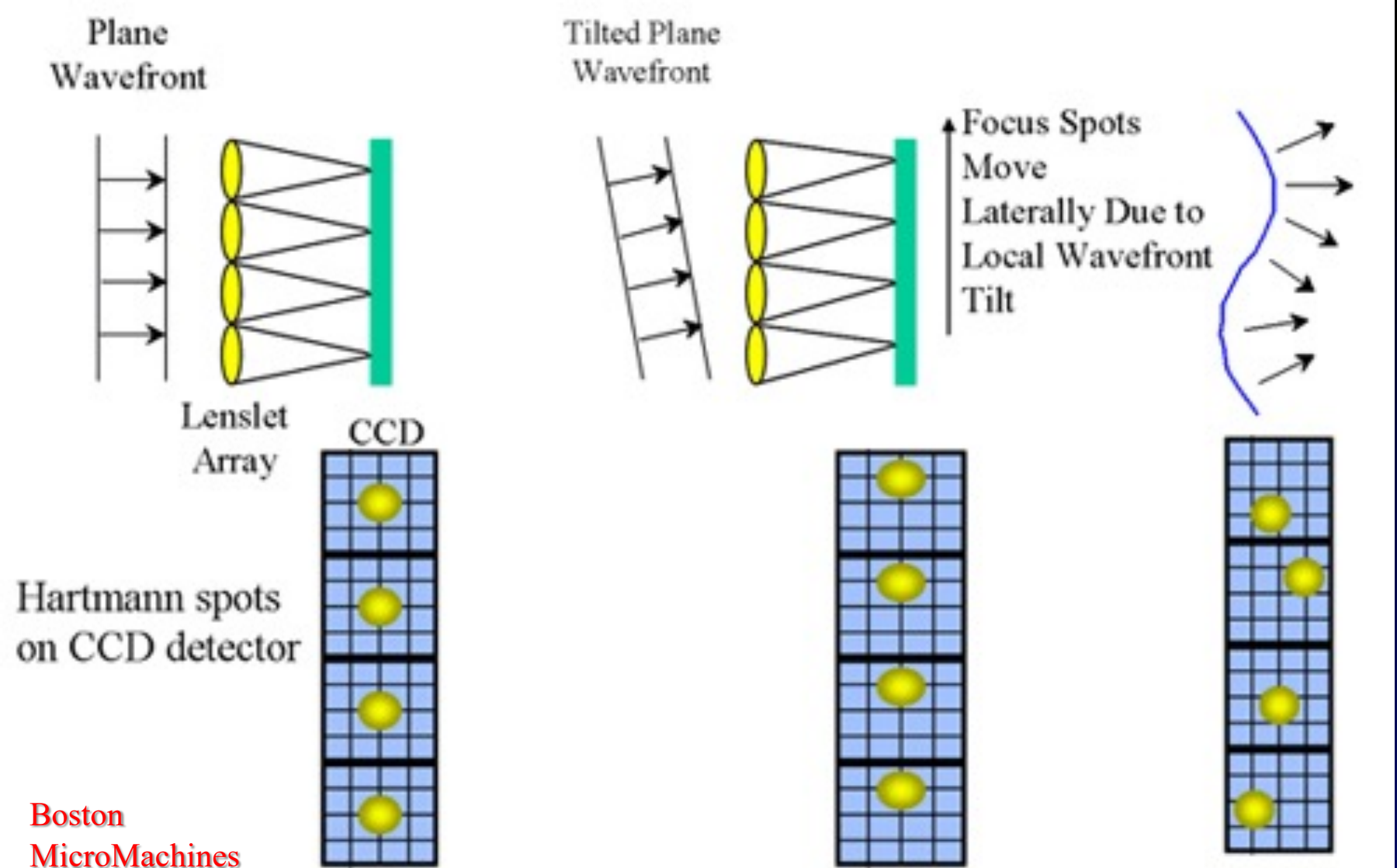


A real demonstration



AO – real time computing and control challenges

- A number of different techniques are used for wavefront sensing, but the simplest conceptually is the Shack-Hartmann sensor
- The pupil is divided into a number of sub-apertures, typically each on the scale of r_0
- the tilt within each subaperture is determined by measuring the centroid of the sub-image – the displacement relative to the unaberrated pupil gives the tilt angle. A global reconstructor then estimates the overall shape
- A signal is applied to the matching actuators in the deformable mirror to counteract the tilt.
- This has to be done before the distortions change significantly



Shack Hartmann WFS: For a large telescope, need 10s of subapertures across the pupil diameter and so the stellar flux from a guide star is divided into 100s or thousands of sub-apertures

Practical Considerations

r_0 the turbulence coherence length, or Fried Parameter, is the typical size of turbulent cells in the atmosphere. Typically 5cm to 20cm in the visible at good sites

Angular isoplanatism – the angular measure over which a compensated wavefront can be considered planar ($< \pi$ radians). At visible wavelengths the isoplanatic angle is about 2 arc seconds increasing to 10 arc seconds in the near infrared.

- Compensation in visible wavelengths (0.5 μ m) requires a guide star of magnitude 10 or brighter.
- Compensation in infrared wavelengths (2.2 μ m) allows guide stars down to magnitude 14.
- Small isoplanatic region around the guide star limits targets
 - Visible – 1/100,000 of the sky
 - IR – 1/1000 of the sky

Strehl

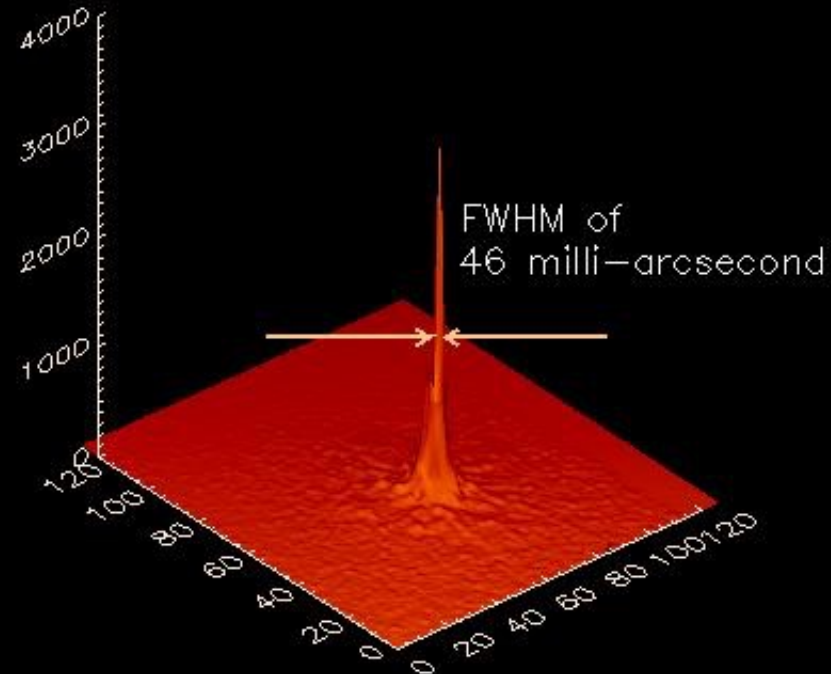
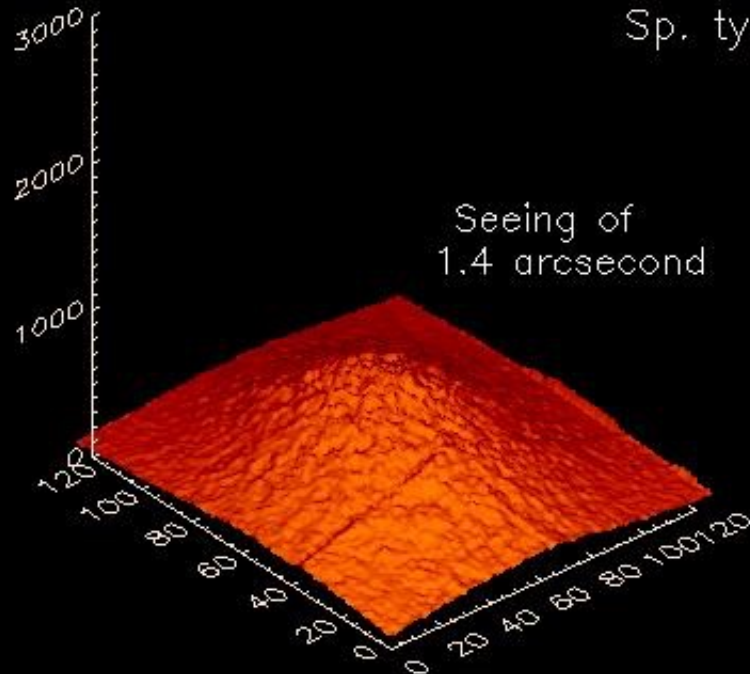
SAO 74164

V mag. = 4.4

Sp. type: G8III

open loop

Keck I AO loop closed



H band images – $1.6\mu\text{m}$
14 Dec 2000 – 07:45 UTC

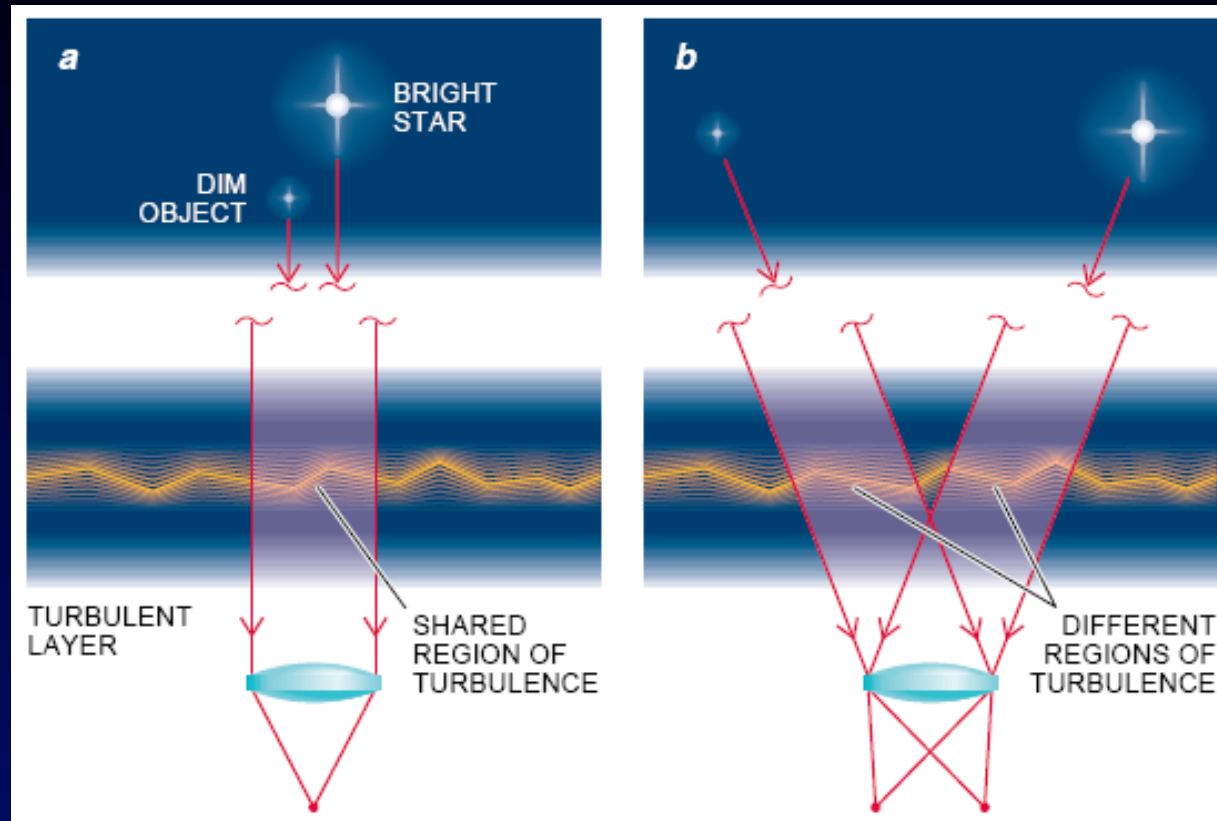
Strehl ratio: 0.23

A measure of the quality of correction is the Strehl ratio – the fraction of intensity contained in the central maximum compared to the theoretical diffraction pattern

Isoplanatic Angle

Where a target is separated from a guide star by a significant angle, the column of turbulence along the path to the two objects diverges and leads to decorrelation.

AO correction falls off rapidly as the separation increases



The definition of the atmospheric isoplanatic angle θ_0 is

$$\theta_0 = 0.31 r_0 / h$$

where h is the characteristic altitude of turbulence

WFS Sensitivity Limits

With frame rates $\sim 1\text{kHz}$, and e.g. 20×20 subapertures, the photon flux/ sample/subaperture is $\sim 10^6$ times lower than the photon flux/sec gathered by the telescope.

The light from each sub-aperture is imaged onto a small number of pixels and needs sufficient signal for the centroid to be measured.

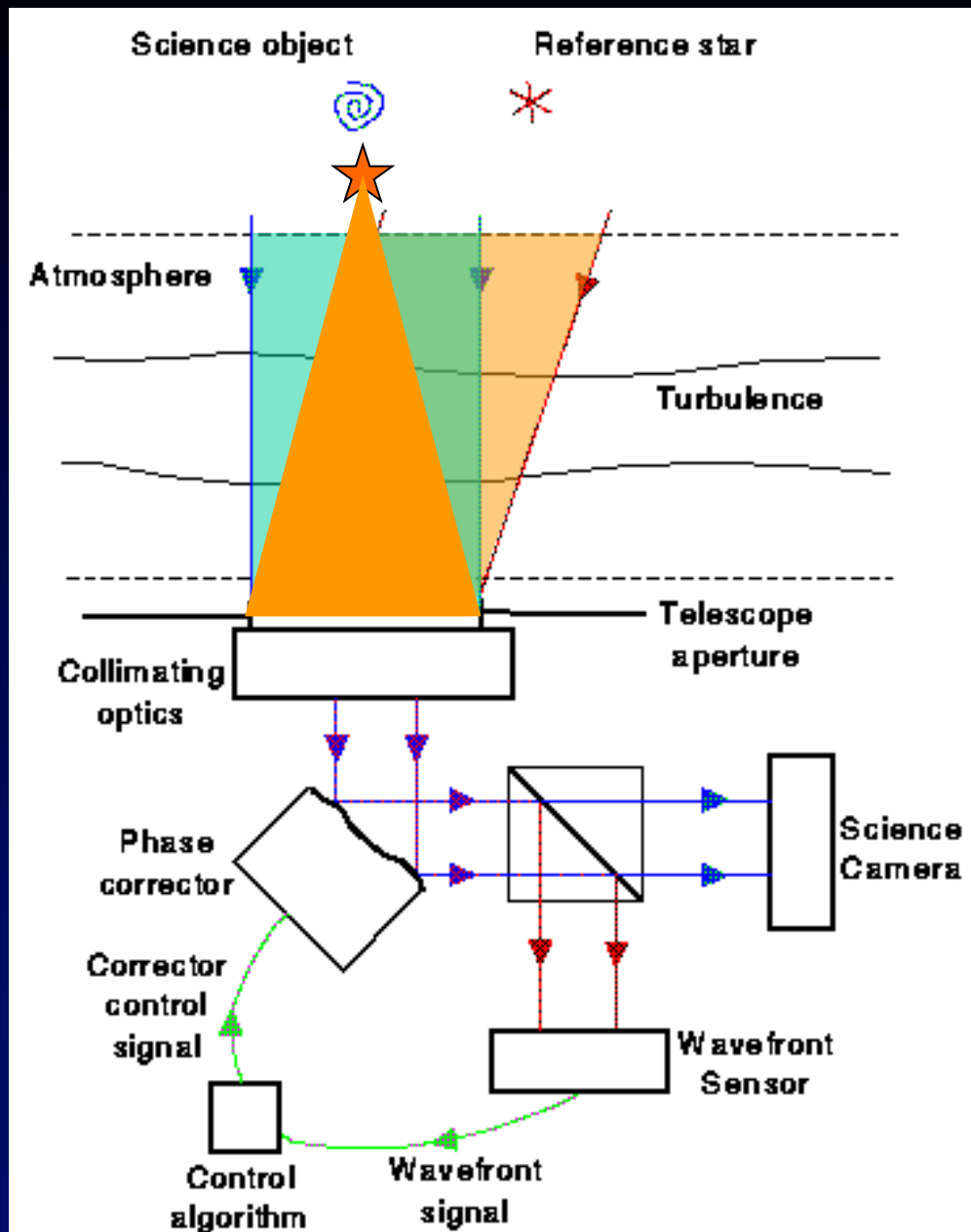
The measurement error depends on the number of detected photons and $\propto 1/\text{SNR}$ so there is a trade off between star brightness and quality of correction

With low-noise detectors, typically require stars of magnitude < 14 as AO guide stars for IR imaging

Twinkle, twinkle, laser star

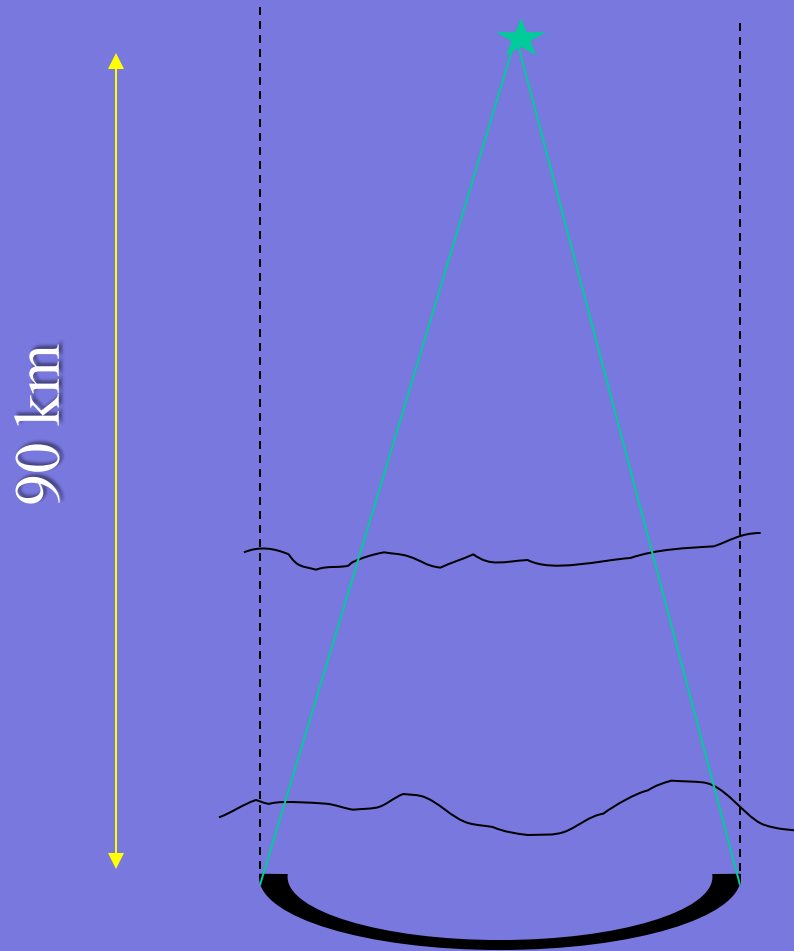


Limitations of Laser Stars



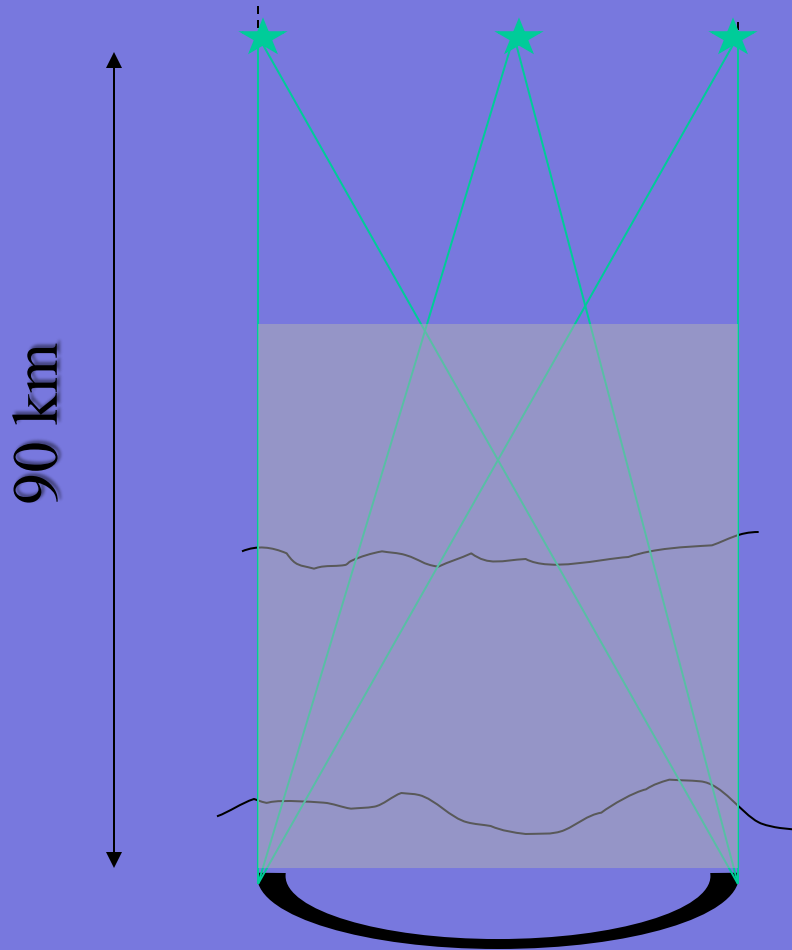
Tomography

1. Cone effect

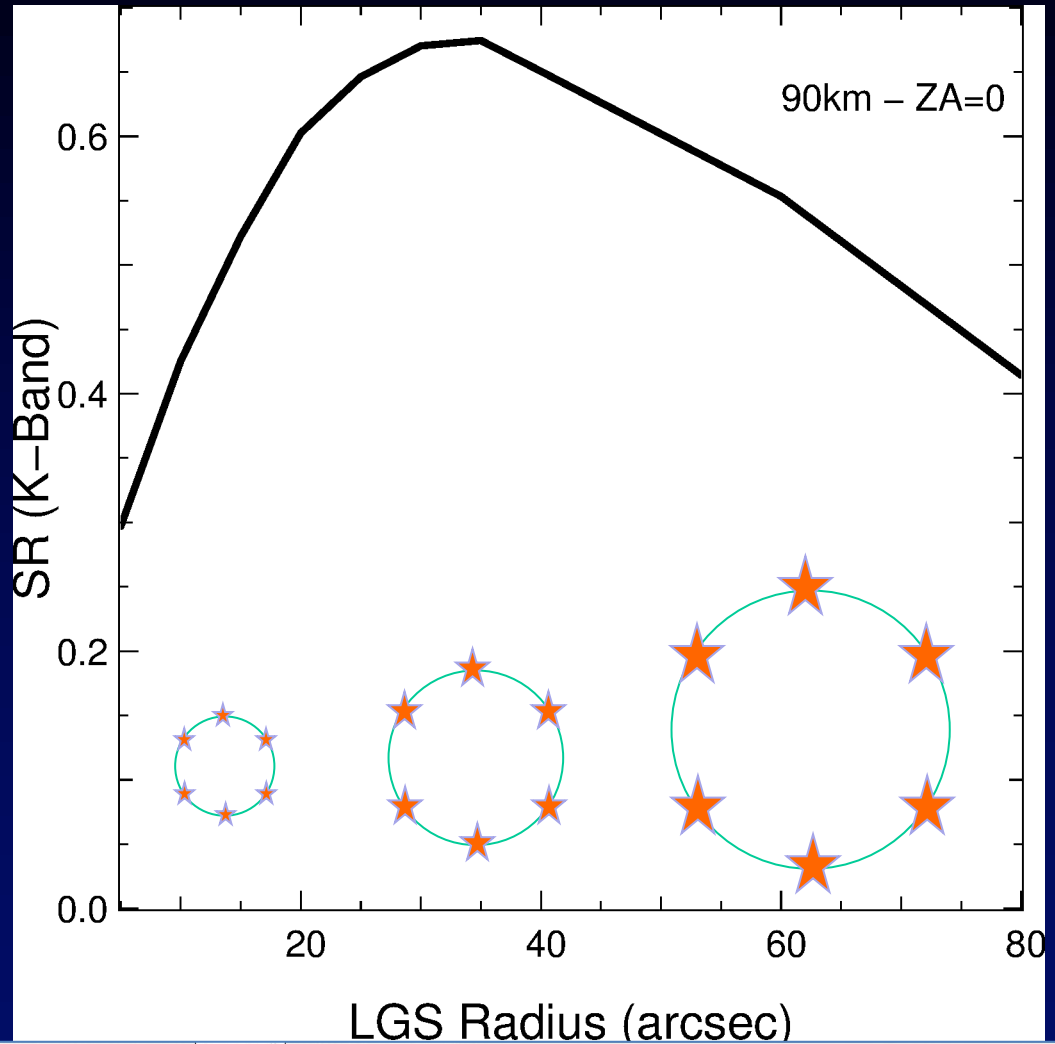


Tomography ?

2. Multiple guide star and tomography

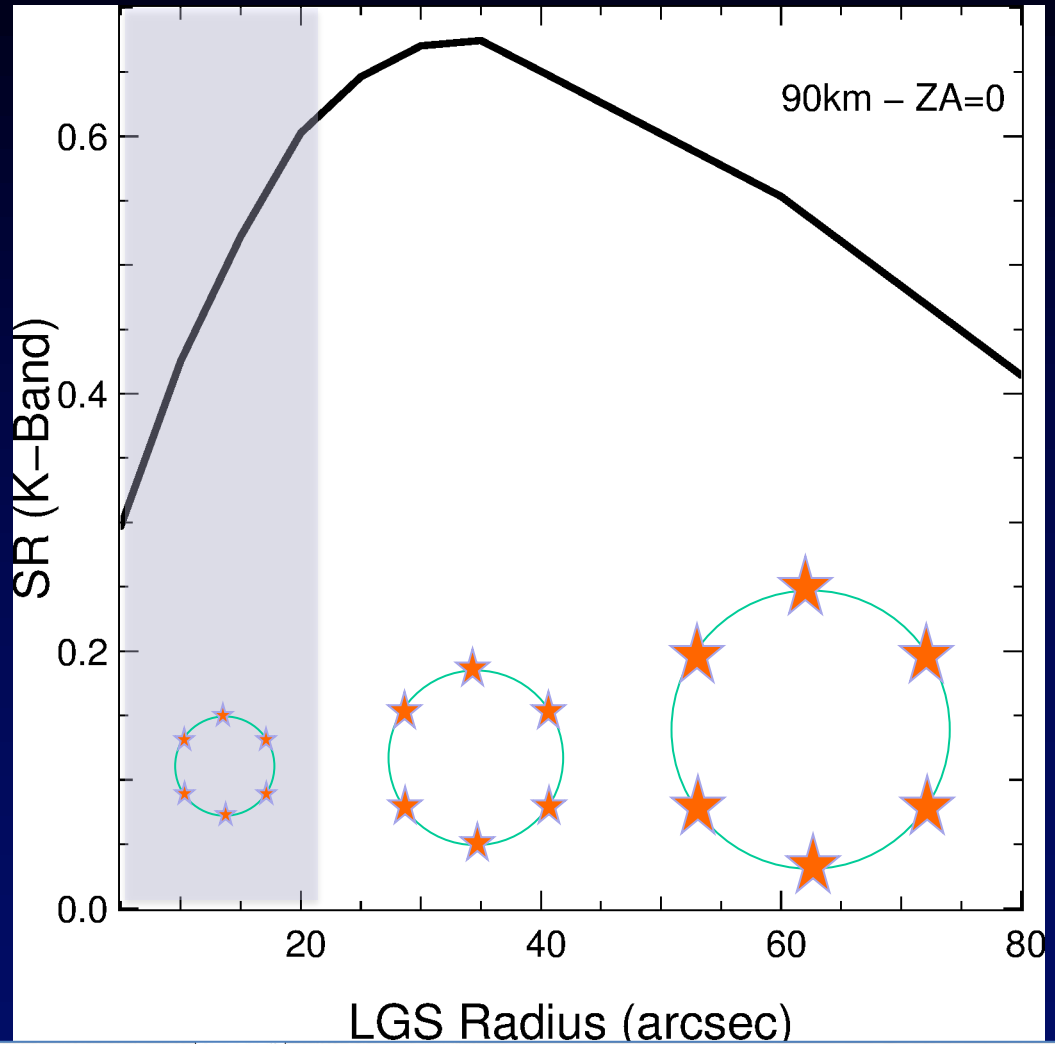


Impact of LGS constellation



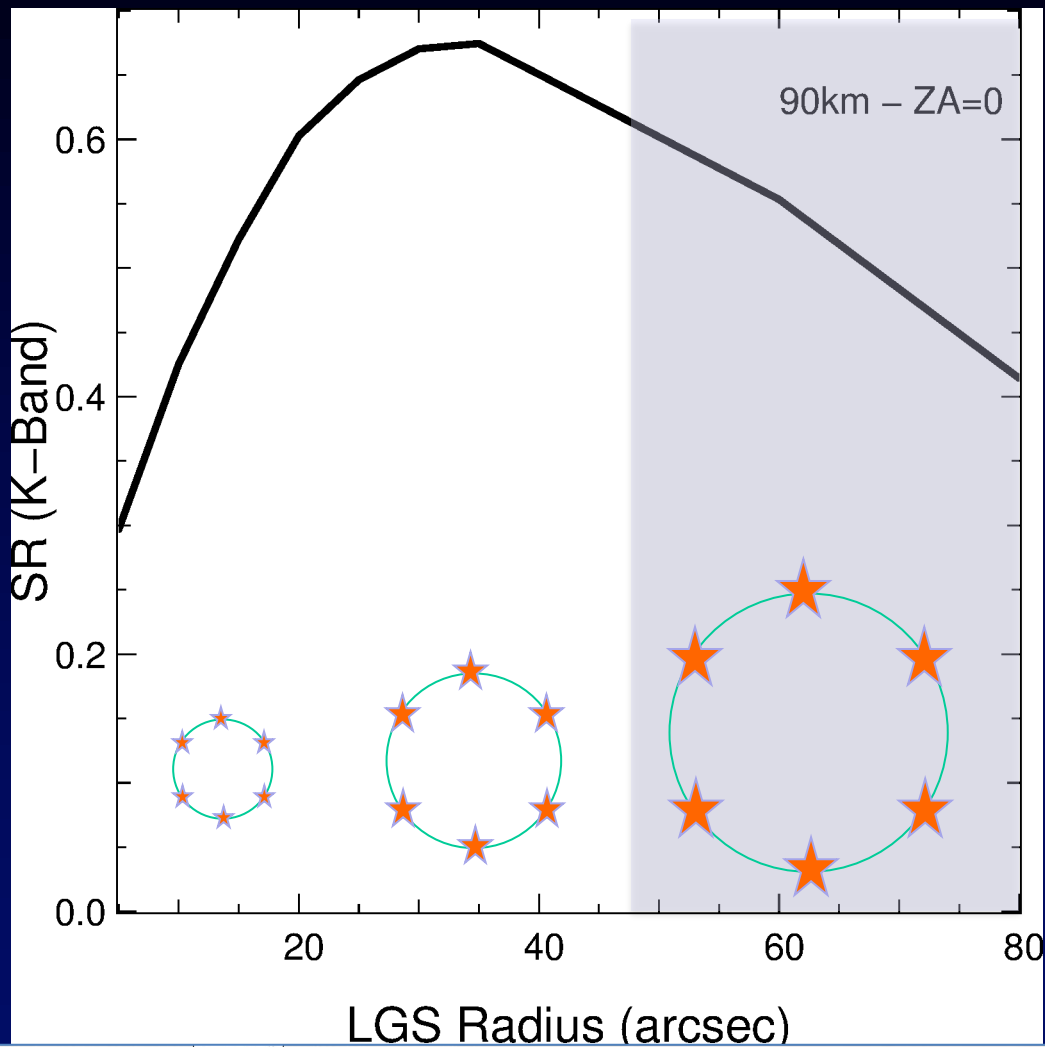
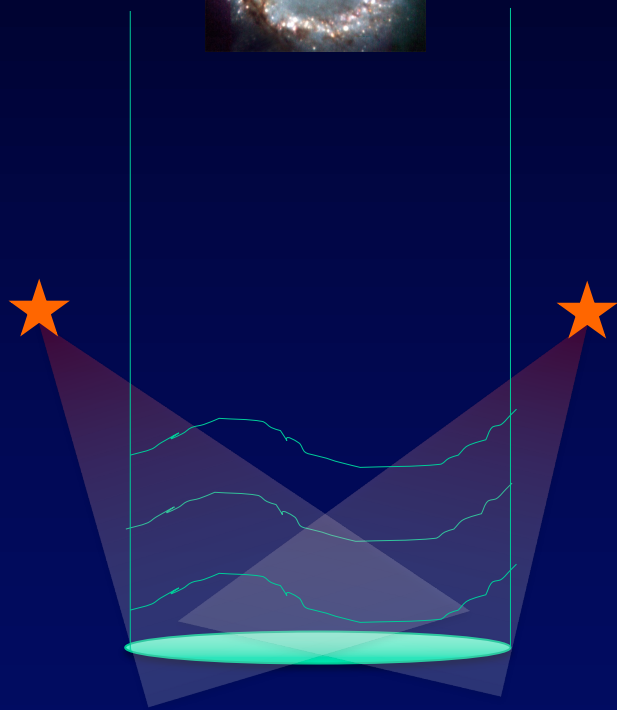
Contribution from Miska Letouarn (ESO - OCTOPUS) and Carlos Correia (OOMAO)

Impact of LGS constellation



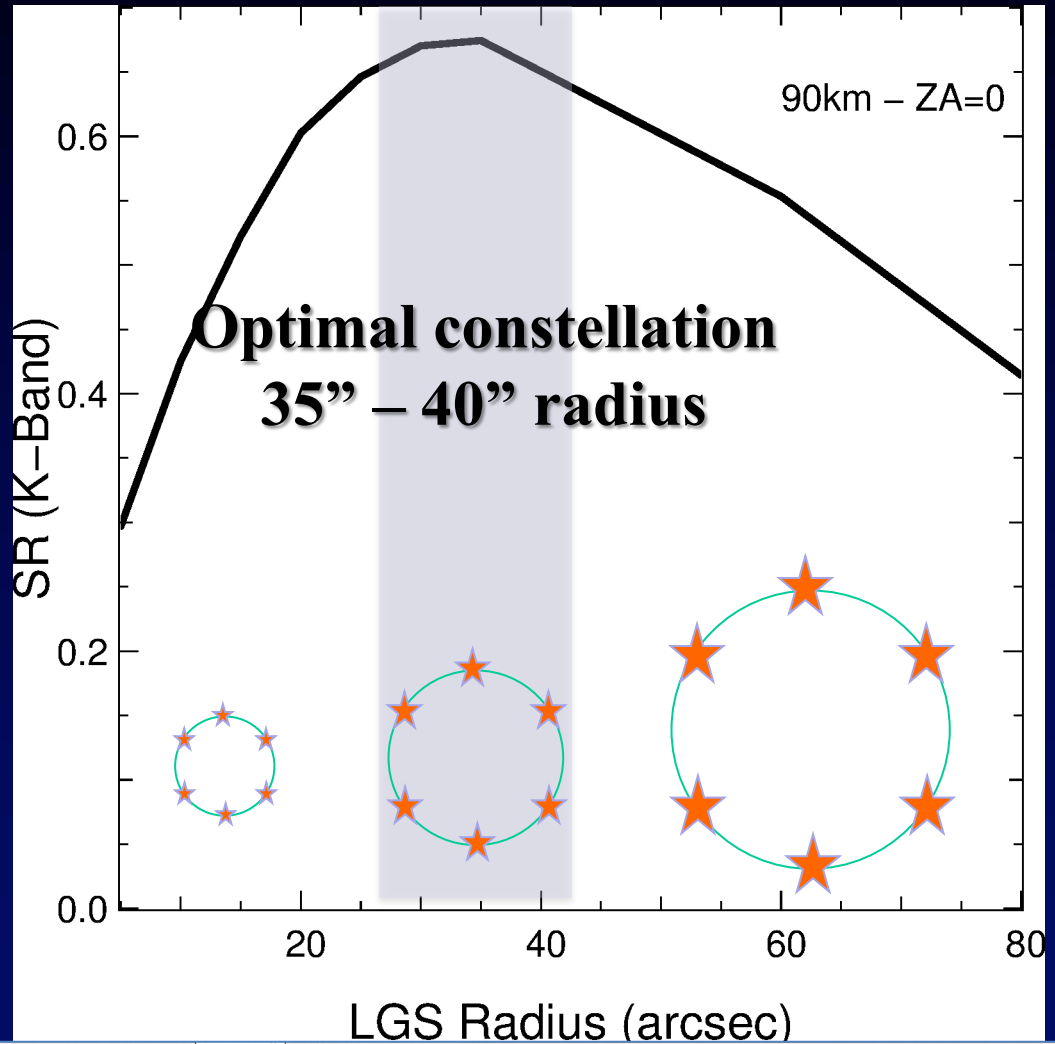
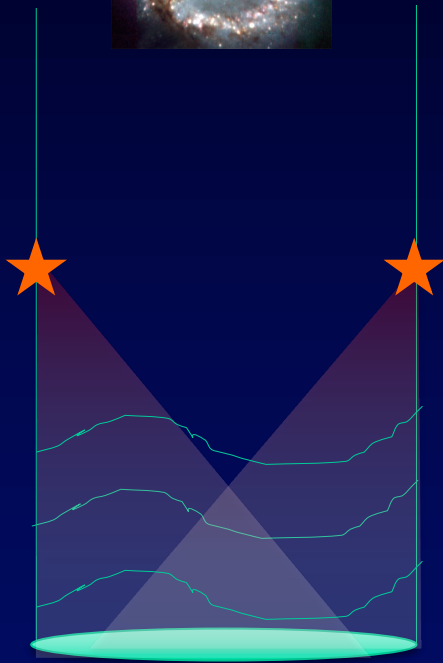
Inspiration from Miska Letouarn (ESO - OCTOPUS) and Carlos Correia (OOMAO)

Impact of LGS constellation



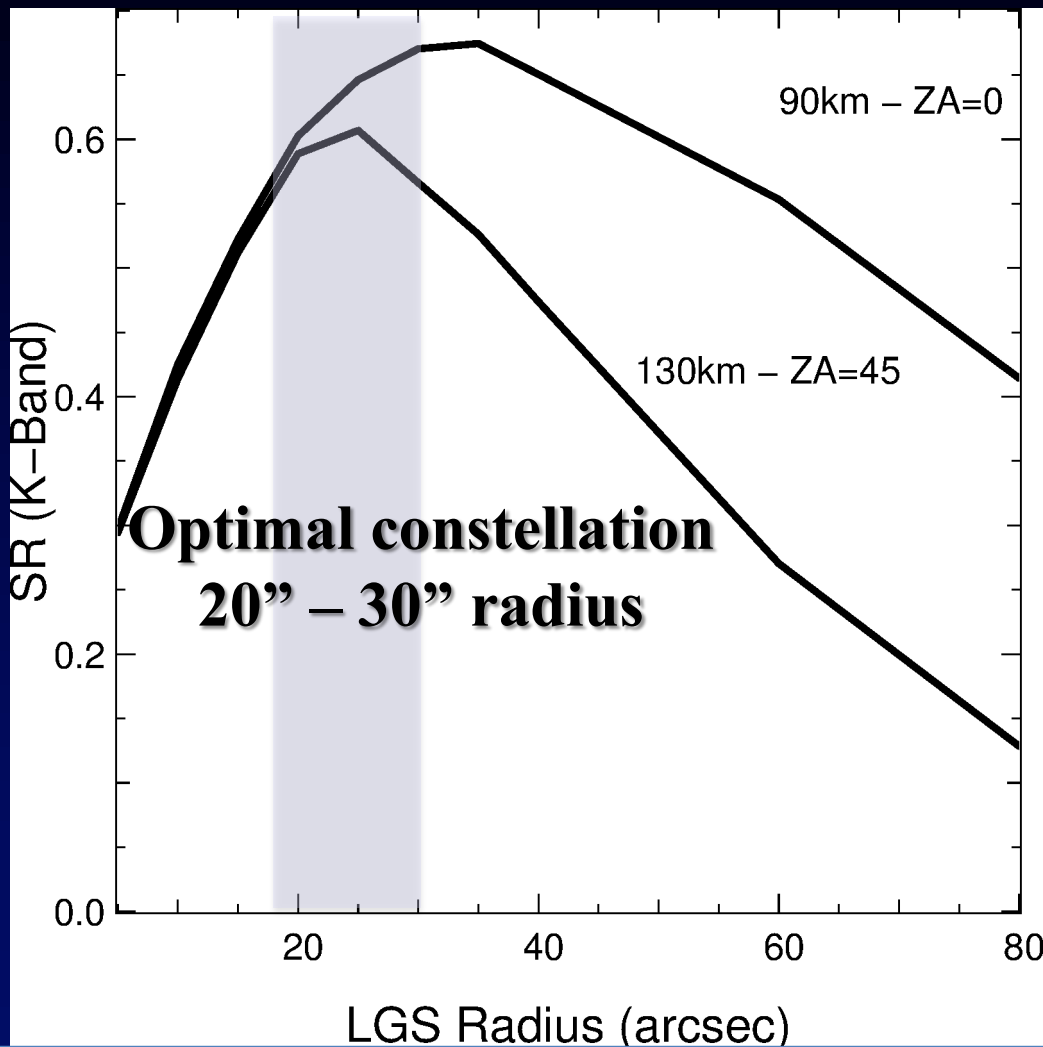
Contribution from Miska Letouarn (ESO – OCTOPUS) and Carlos Correia (OOMAO)

Impact of LGS constellation

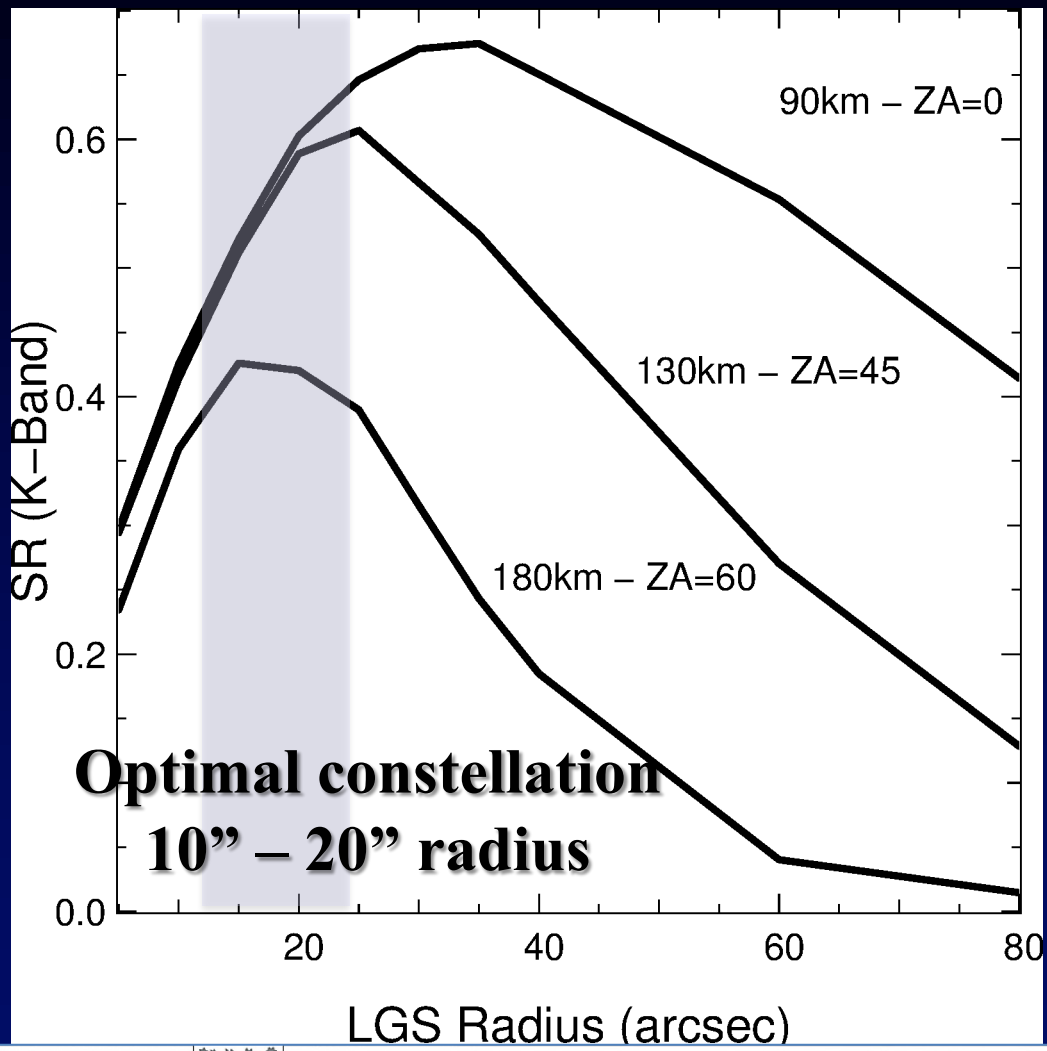
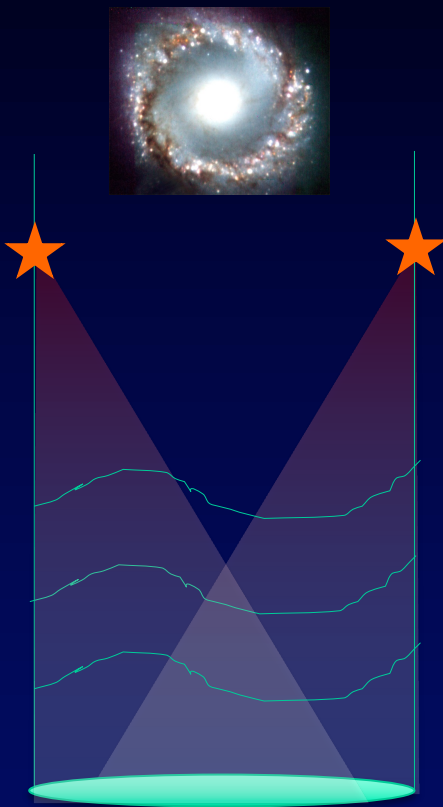


Support from Miska Letouarn (ESO - OCTOPUS) and Carlos Correia (OOMAO)

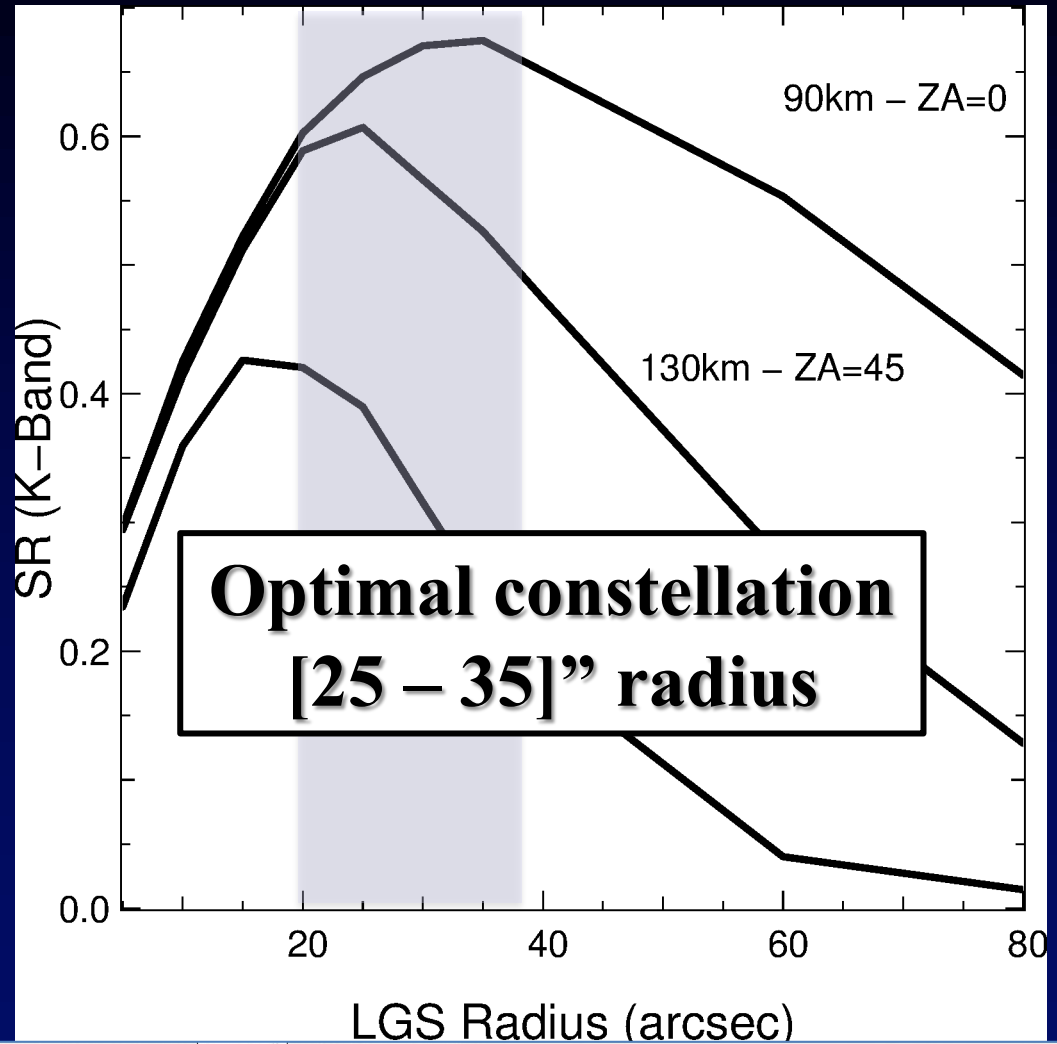
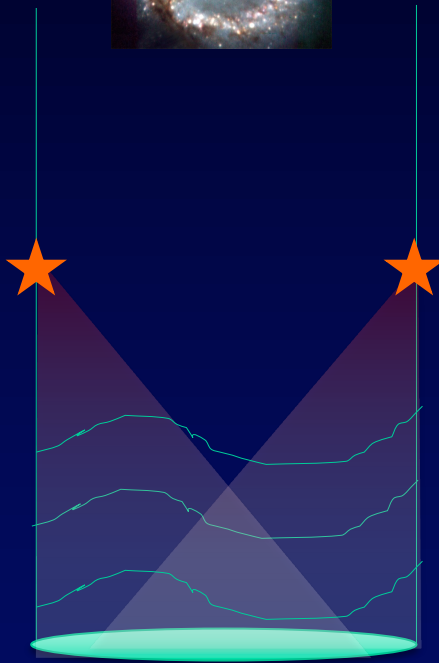
Impact of LGS constellation



Impact of LGS constellation



Presented by Miska Letouarn (ESO – OCTOPUS) and Carlos Correia (OOMAO)



Contribution from Miska Letouarn (ESO – OCTOPUS) and Carlos Correia (OOMAO)

Limitations of Laser Stars

The laser beam passes through the atmosphere up to the sodium layer and the tilt component causes the position of the star to wander.

A natural guide star is used as the tilt component reference.

The cone of light from the LGS samples a subset of the cylinder that the telescope beam encompasses so it does not cover some turbulence : focal anisoplanatism or the Cone effect

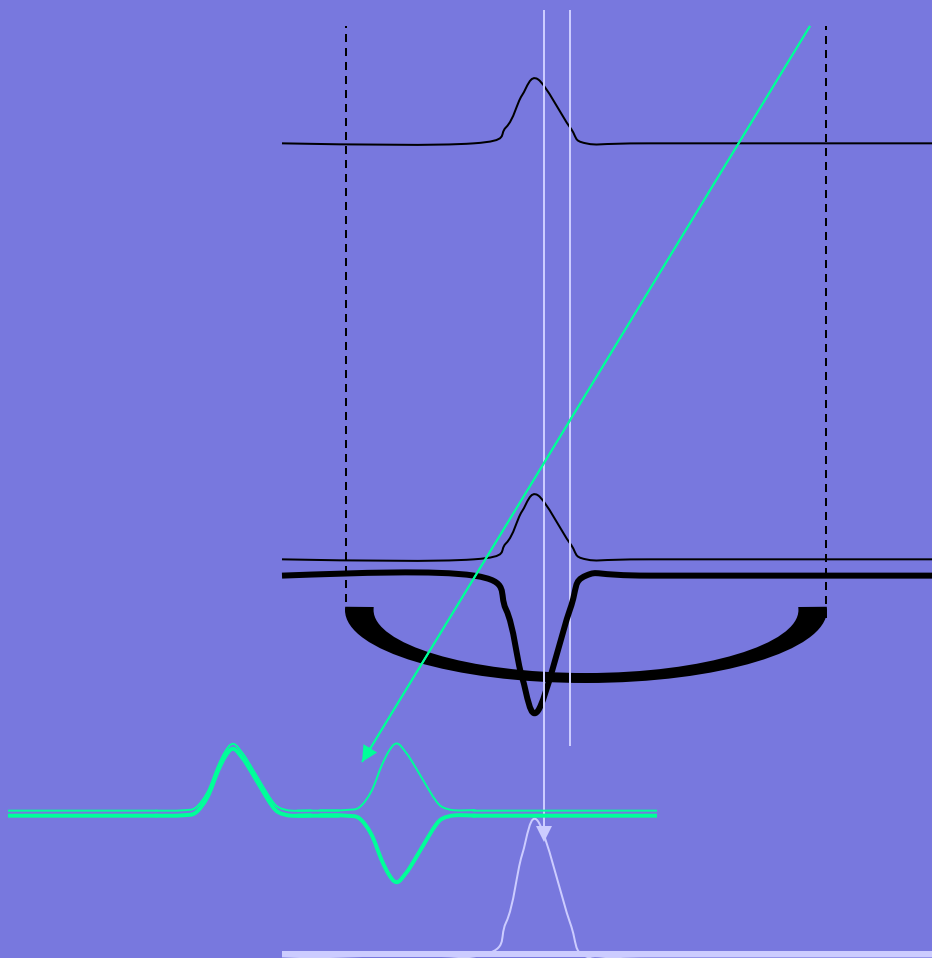
Produces ~ 2 arcsec 'star' at zenith, which is elongated at higher airmass due to Na layer thickness.

The distance to the sodium layer increases with zenith distance, so continuous refocussing or path length compensation is required.

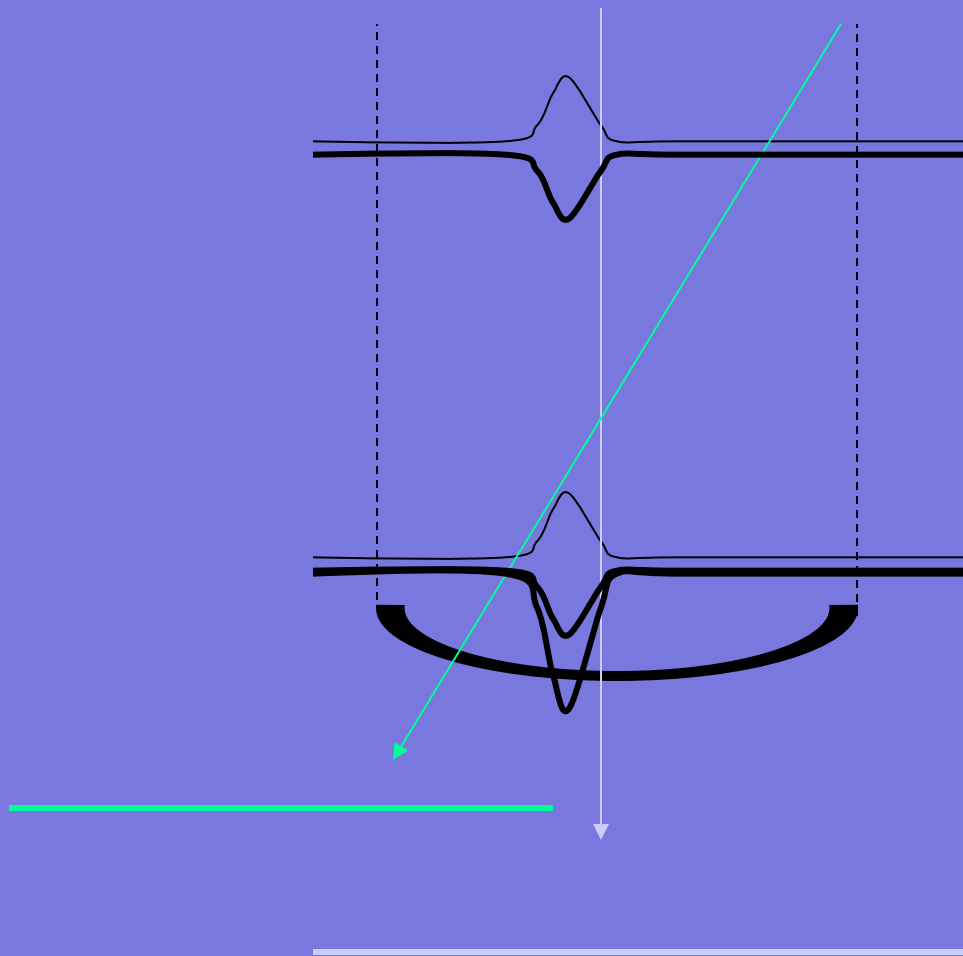
Advanced AO

- 4 (or more) LGS in a constellation can cover the full cylinder and give improved correction
- Combined with multiple deformable mirrors (DMs), conjugated to different altitudes, this gives complete sampling and improved correction for the atmosphere.
- Multi-conjugate AO - e.g GEMS at Gemini-S
- Xtreme AO with high density actuators to give very high strehl images – e.g for exoplanet searches

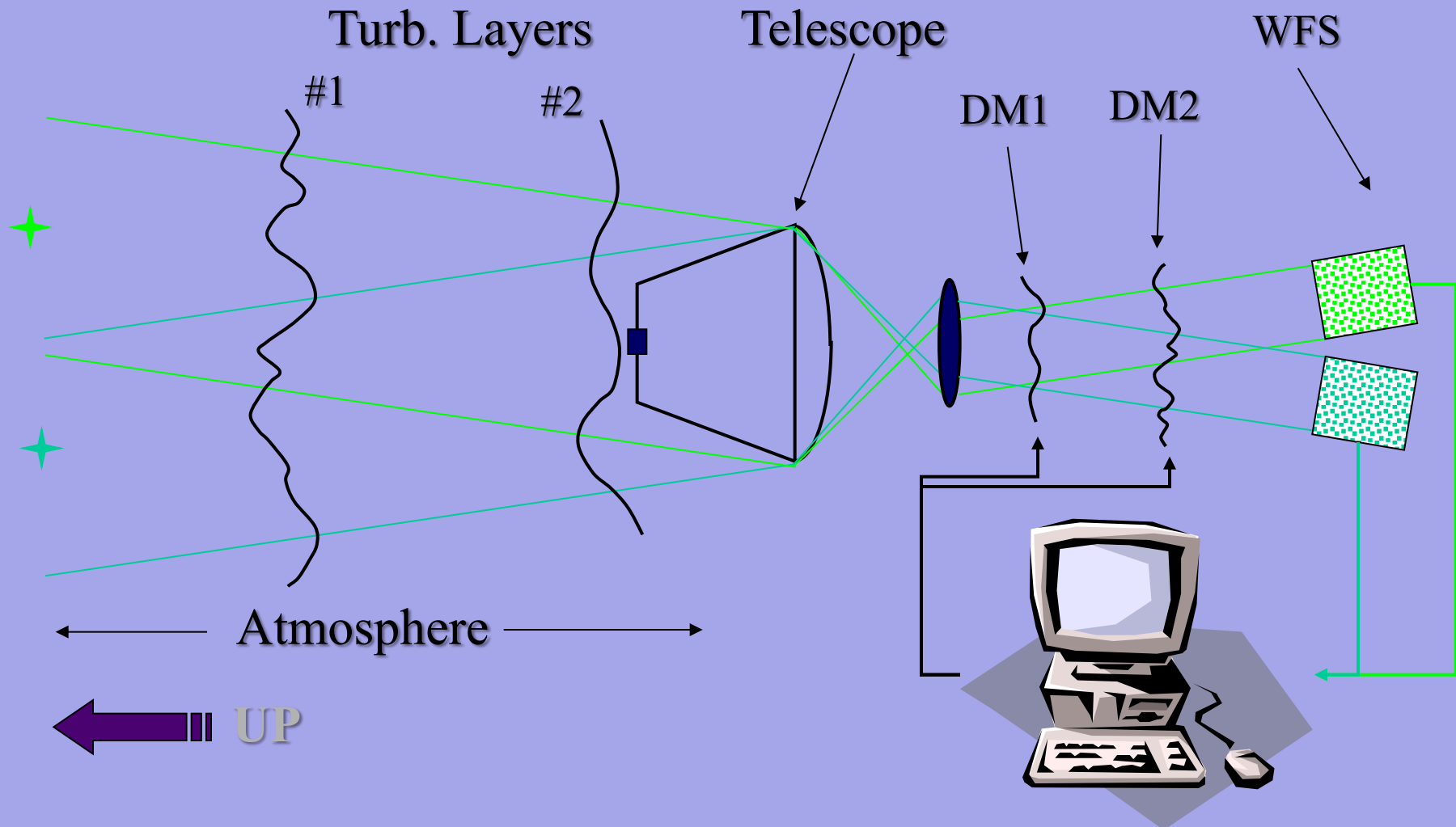
Multiconjugate



What is multiconjugate?



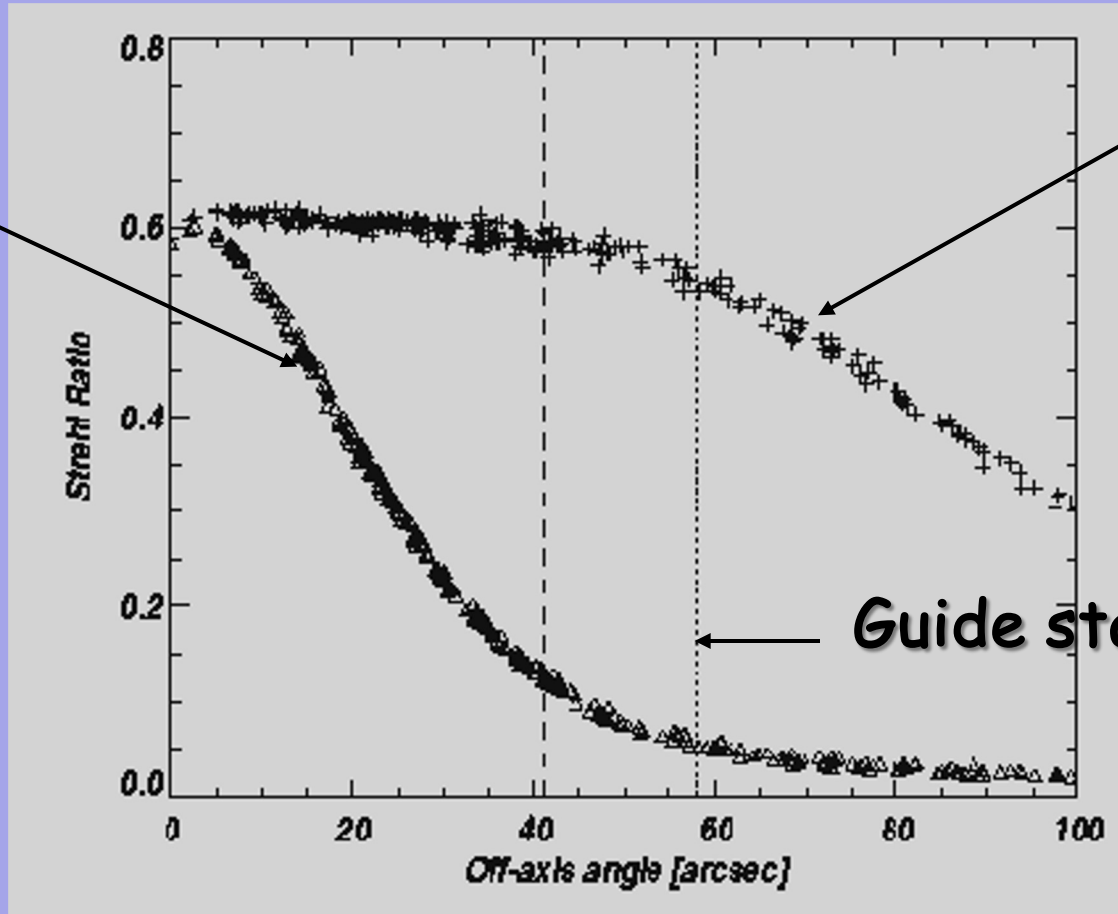
Multiconjugate AO



MCAO Performance Summary

Early NGS results, MK Profile

Classical AO



MCAO

Guide star location

Laser Guide Stars

Substantial development programmes in sodium lasers, wavefront sensors, deformable mirrors, reconstructors and control systems

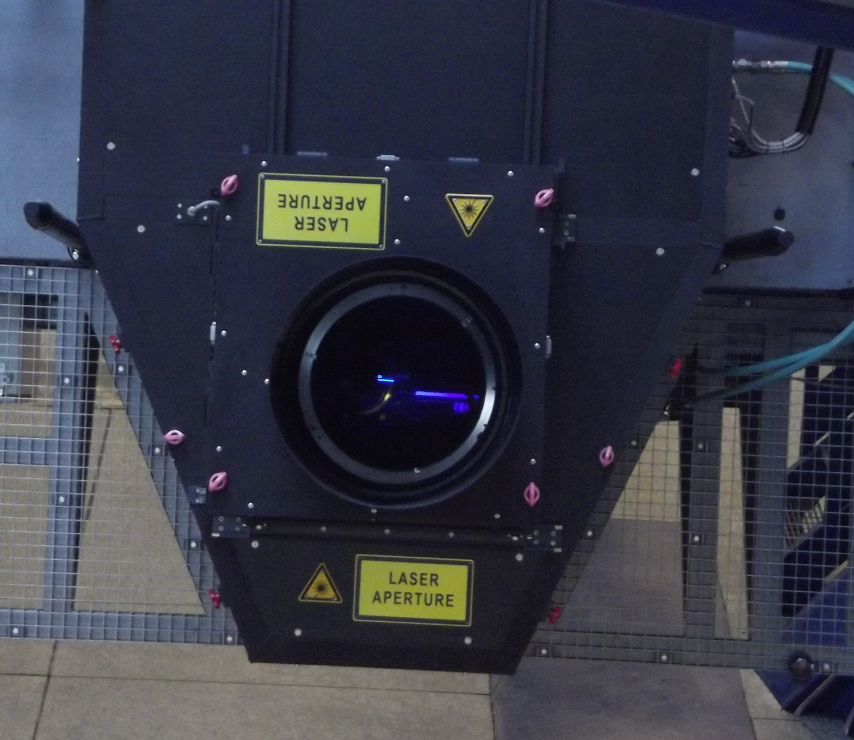
GEMS : LGS MCAO system on Gemini-S feeding GSAOI (Infrared AO Imager) or FLAMINGOS (IR Multi-object Spectrometer)

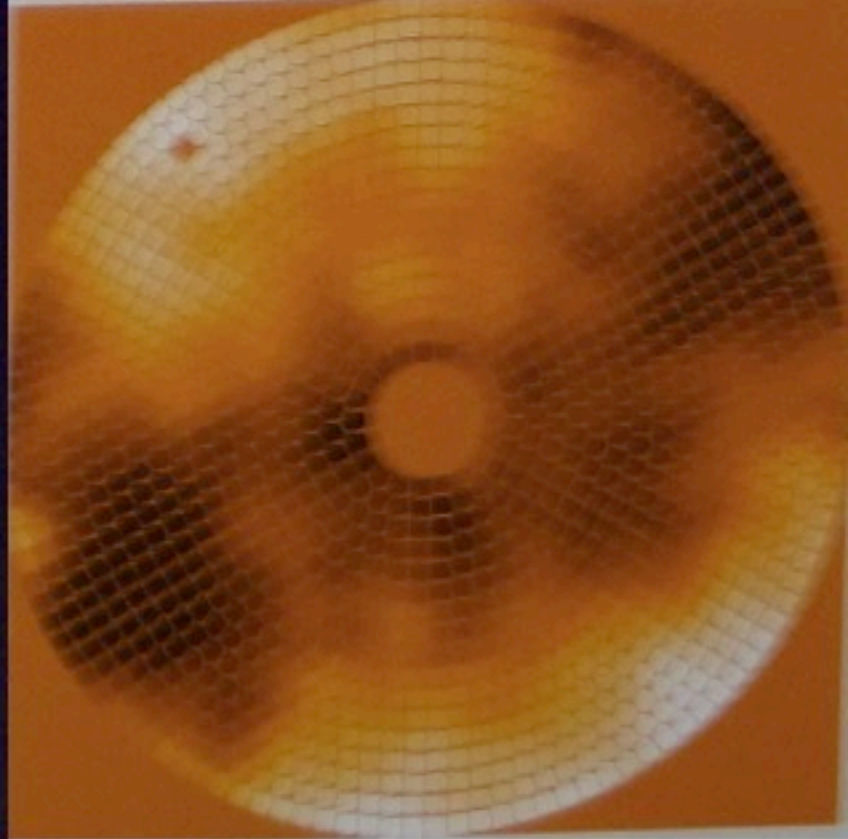
VLT AOF on UT4 is operating at Paranal feeding Hawk-I or MUSE



Gemini Observatory Legacy Image

VLT UT4 Laser launch telescopes

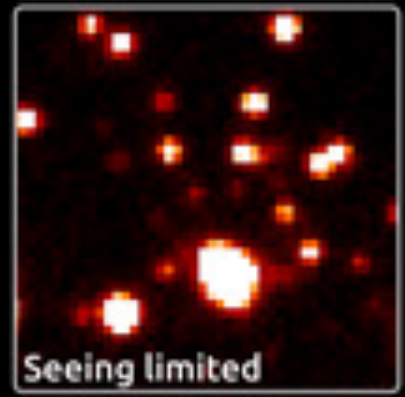
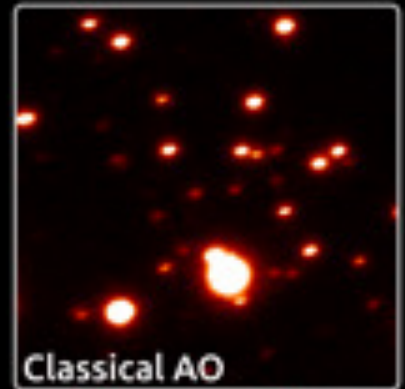
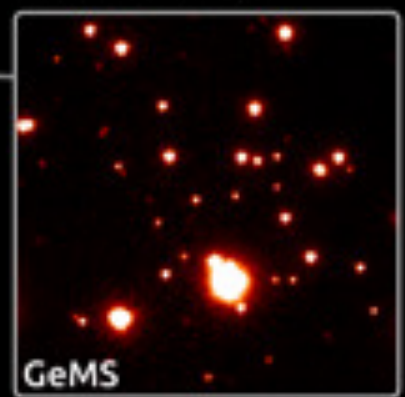
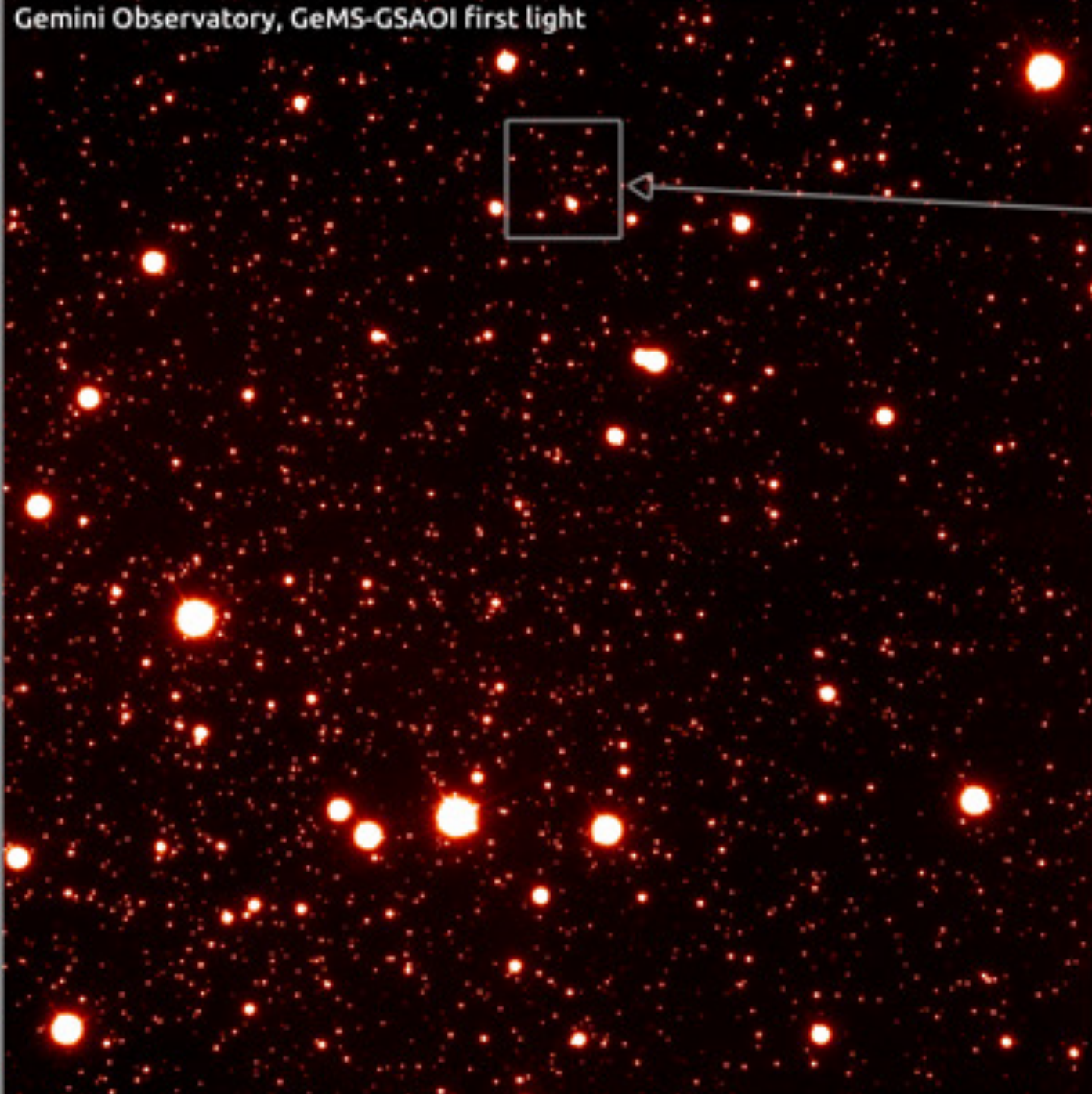




The LGS constellation produced by the adaptive Optics Facility at the UT4 telescope of the ESO VLT. Light from the LGS is used to estimate the wavefront distortions and corrections are applied to the deformable secondary mirror. The image above shows a snapshot of the phase corrections applied to the secondary.

Gemini Observatory, GeMS-GSAOI first light

NGC288, H band
13mn exposure
Field of View 87"x87"
FWHM = 0.080"
FWHM rms = 0.002"



GeMS

Classical AO

Seeing limited

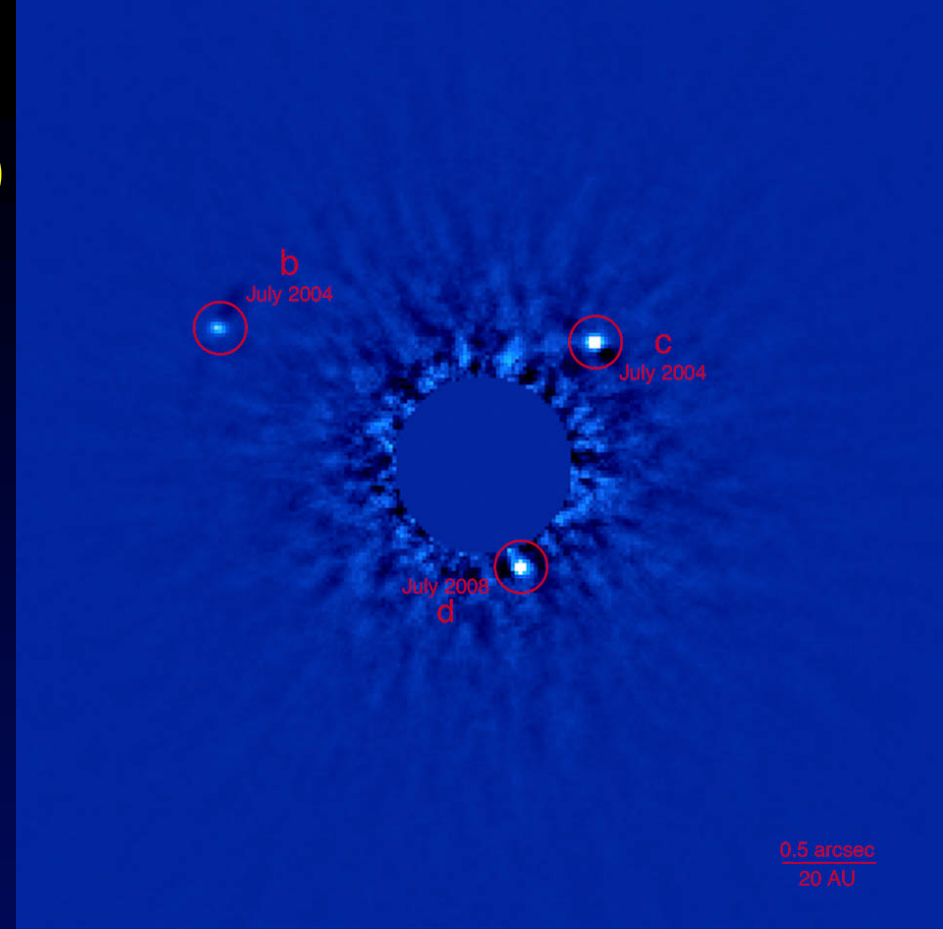
Different AO Flavours

Method		Corrected field of view
Laser Tomography AO	LTAO	10's of arc sec
Multi-Object AO	MOAO	N x 10's of arc sec
Multi-Conjugate AO	MCAO	≤ about 2 arc min
Ground Layer AO	GLAO	A few to 10 arc min

+ Extreme AO - aimed at very high Strehl on bright Natural Guide Stars – exoplanet searches

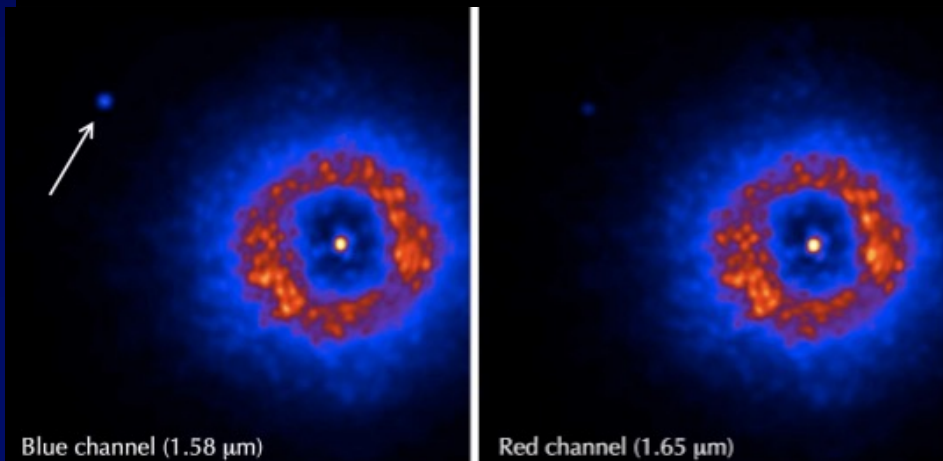
Challenges of AO

- Improved resolution, sharper images, but quite variable temporally and spatially, so calibration is tricky
- MCAO helps but is not widely available
- Uncorrected modes may still be significant, and often techniques such as Angular or Spectral Differential imaging are used to improve the subtraction of these effects (ADI or SDI).
- AO may be used with a coronagraph to suppress the light from the host star



Gemini Observatory / NRC / AURA / Christian Marois, et al.

Gemini Observatory Legacy Image



ADI (Angular Differential Imaging) + SDI (Spectral Differential Imaging)

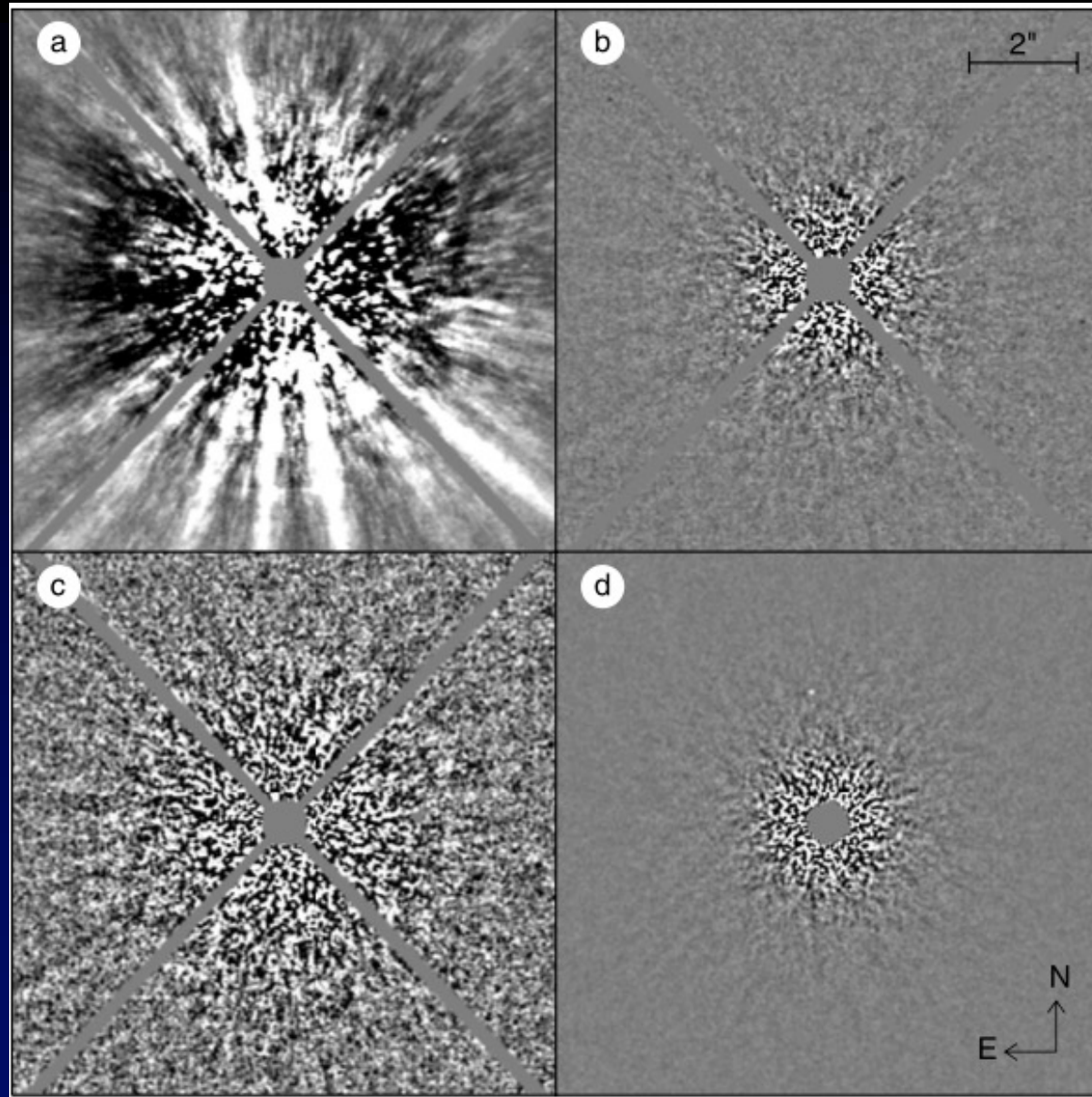
- Residual image structure is partially due to aberrations in the telescope and instrument and uncorrected atmospheric structure
- In Angular Differential Imaging, a sequence of many exposures of the target is acquired using an altitude/azimuth telescope with the instrument rotator turned off (at the Cassegrain focus) to keep instrument and telescope optics aligned.
- This is a very stable configuration and ensures a high correlation of the sequence of PSF images, which would be smeared out if the rotator was used.
- The FOV rotates during the sequence, which has to be allowed for after subtraction of a reference image.
- Spectral Differential Imaging uses images obtained simultaneously on and off a spectral feature (e.g. the 1.6 μ m methane absorption) where the aberrations are highly correlated because they are very close in wavelength
- Spectral deconvolution can be applied to spectrally dispersed Integral Field images (e.g. Thatte et al 2007). Here speckles and other aberrations increase in distance as a function of wavelength because of the increasing diffraction angle, but the separation of an object from its host star is at a fixed distance.

ADI illustrated with Gemini NIRI/Altair 1.6 μ m observations (Lafreniere et al 2007)

(a) Original 30s image of the young star HD 691 after subtraction of an azimuthally symmetric median intensity profile.

(b and c) Corresponding residual image after ADI subtraction using the LOCI algorithm. . Display intensity ranges are 5×10^{-6} and 10^{-6} of stellar PSF peak for the top and bottom rows, respectively

(d) Median combination of 117 such residual images. Each panel is $10''$ on a side. The diffraction spikes from the secondary mirror support vanes and the central saturated region are masked. The faint point source visible in (d) at separation of $2.43''$ could not have been detected without ADI processing.



Spectral Deconvolution

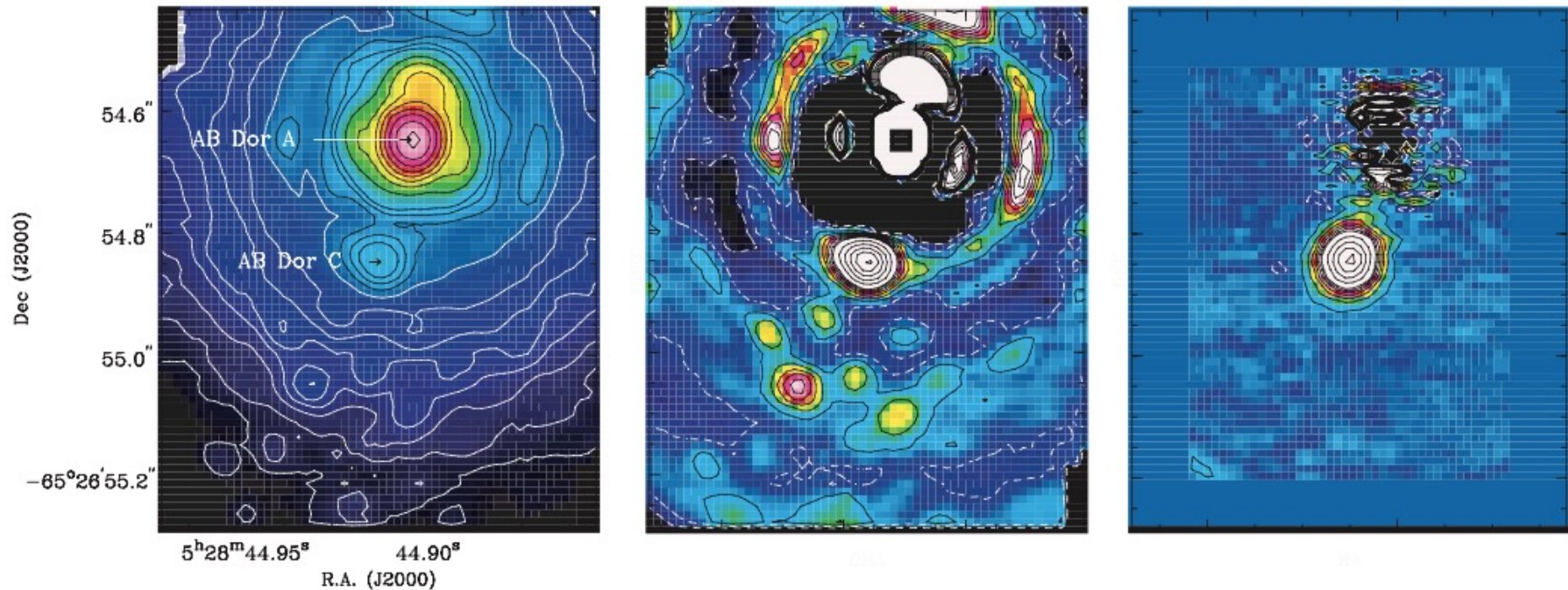
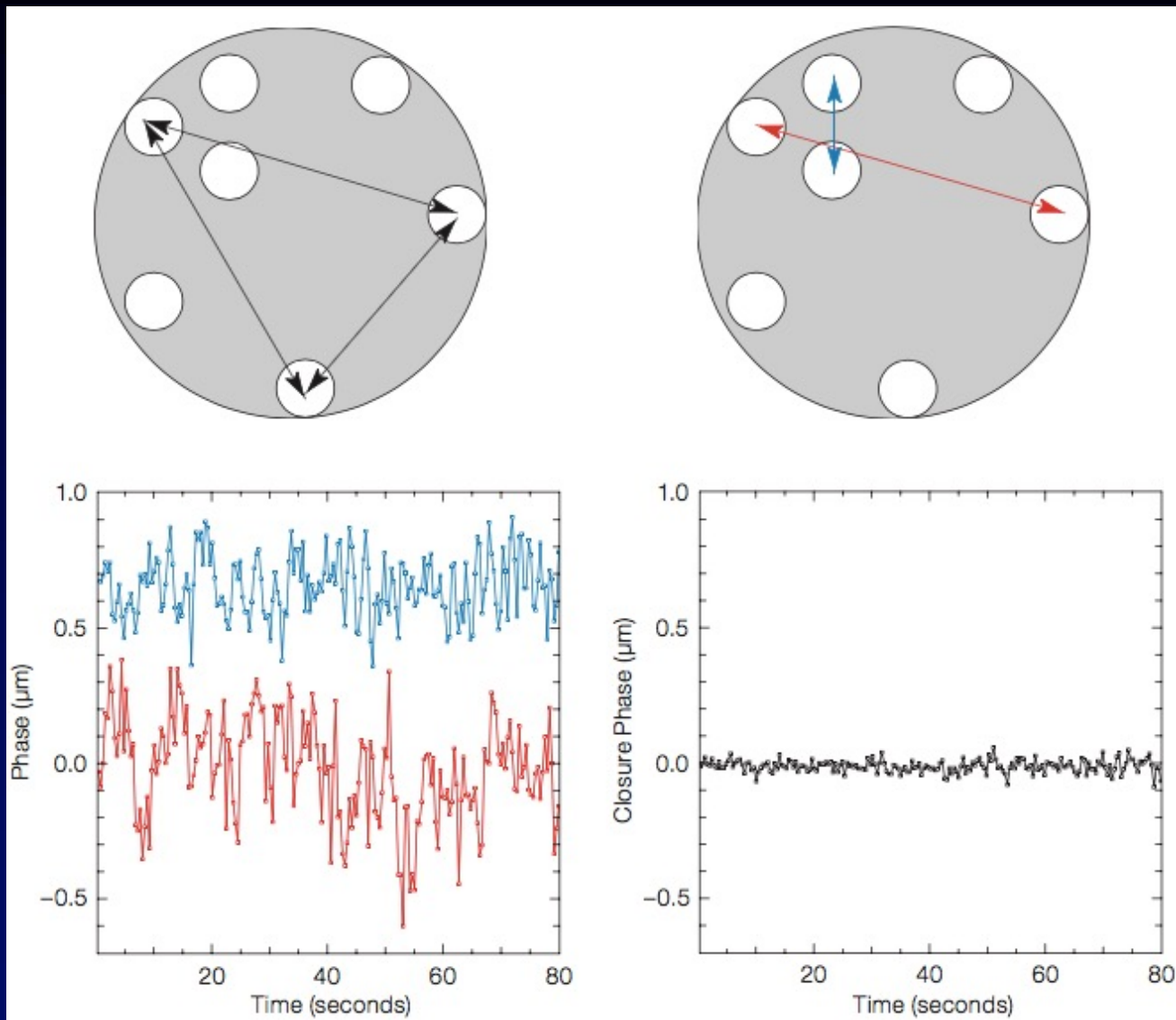


Figure 2. Illustration showing the efficacy of the SD technique at removing both PSF artefacts and super-speckles from the SINFONI IFS data cube for the AB Dor system. The left-hand frame shows one wavelength slice of the observed data cube at 2.2 μm . Note that the entire vertical extent of the image is only 0.9 arcsec. The colour table is logarithmic (minimum 10^1 , maximum 10^4). The contours are logarithmic, from 0.9 to 2.3 in steps of 0.1, and from 2.3 to 4.0 in steps of 0.2. The middle frame shows the same data, but with a radial profile fitted and subtracted, so as to highlight the PSF imperfections. The super-speckles are easily confused with real sources in this narrow-band image. The colour table is now linear (minimum -10 , maximum 25), with contours from -12.5 to 32.5 in steps of 5, and from 32.5 to 150 in steps of 20. The four-fold symmetry of the Airy pattern arises from the superposition of the diffraction spikes of the secondary support structure on the Airy rings. The right-hand frame shows the same wavelength slice of the data cube, after applying the SD technique iteratively. Colour table and contours are the same as for the middle frame. Super-speckles are completely absent at the lowest contour level of ± 2.5 , corresponding to a 1σ error of ≤ 1 unit.

Thatte et al 2007

Sparse Aperture Mask Interferometry

Phase differences from a mask in NACO on the VLT data are shown in the lower left panel for two different pairs of holes (red and blue baselines, marked on the pupil image), exhibiting phase residuals of ~ 300 nm. In the lower right panel, the closure phase - the sum of three phases of three baselines formed by three separate holes (the triangle is given by black arrows in the pupil image) is given. Most of the phase noise from uncorrected seeing disappears, leaving a closure phase residual of 10 nm; an improvement by a factor of 30.

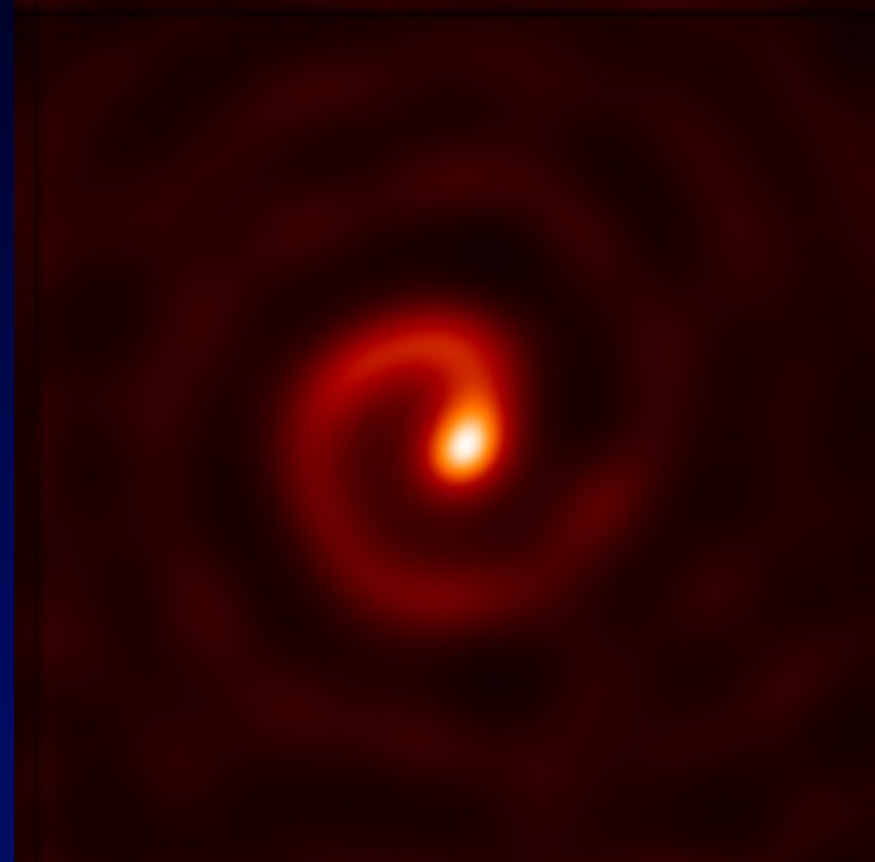


. (Lacour et al 2011)

Sparse Aperture Masking

SAM uses only a fraction of the light collected by the telescope, but provides enhanced stability and resolution, making it suitable for bright objects on large telescopes

This movie shows a sequence of 11 images of WR104, a late type dusty binary W-R star system obtained on the Keck 10-m telescope in the K-band. (P Tuthill et al 2008)



0.4 arcsec